Mon. Not. R. Astron. Soc. **319**, 721–727 (2000)

In-shock cooling in numerical simulations

Roger M. Hutchings★ and Peter A. Thomas
Astronomy Centre, University of Sussex, Falmer, Brighton BN1 9QJ

Accepted 2000 May 13. Received 2000 May 13; in original form 1999 March 22

ABSTRACT

We model a one-dimensional shock-tube using smoothed particle hydrodynamics and investigate the consequences of having finite shock-width in numerical simulations caused by finite resolution of the codes. We investigate the cooling of gas during passage through the shock for three different cooling regimes.

For a theoretical shock temperature of 10^5 K, the maximum temperature of the gas is much reduced. When the ratio of the cooling time to shock-crossing time was 8, we found a reduction of 25 per cent in the maximum temperature reached by the gas. When the ratio was reduced to 1.2, the maximum temperature reached dropped to 50 per cent of the theoretical value. In both cases the cooling time was reduced by a factor of 2.

At lower temperatures, we are especially interested in the production of molecular hydrogen, and so we follow the ionization level and H_2 abundance across the shock. The effect of in-shock cooling is substantial: the maximum temperature the gas reaches compared with the theoretical temperature is found to vary between 0.15 and 0.81, depending upon the shock strength and mass resolution. The downstream ionization level is reduced from the theoretical level by a factor of between 2.4 and 12.5, and the resulting H_2 abundance by a factor of 1.35 to 2.22.

At temperatures above 10^5 K, radiative shocks are unstable and will oscillate. We find that the shock jump temperature varies by a factor of 20 because of these oscillations.

We conclude that extreme caution must be exercised when interpreting the results of simulations of galaxy formation.

Key words: hydrodynamics – shock waves – methods: numerical.

1 INTRODUCTION

For hydrodynamics codes to be able to simulate shocks, it is necessary that the width of the shock be spread over a few mesh cells, or represent a few interparticle spacings, depending on whether a grid- or particle-based code is being used. In reality, however, the true width of the shock is only a few mean free paths, giving a shock thickness of

$$\Delta x \sim \frac{1}{n\sigma}, \tag{1}$$

where n is the number density, and σ is the collisional cross-section. A few simple calculations show that the true shock thickness is orders of magnitude smaller than the shock thickness obtained in simulations. This allows the possibility that gas in simulations can cool artificially while passing through a shock, and that temperature-sensitive quantities such as ionization levels and molecular abundances may also vary. In this paper we consider a number of possibilities. First, if gas is able to cool during a shock, the maximum temperature, the gas will reach after passing through the shock will be reduced from that of an adiabatic jump. Where the cooling rate decreases with increasing temperature, this may significantly reduce the cooling time of the post-shock gas. Secondly, we shall consider the evolution of the ionization level through a shock, where the cooling rate is proportional to the number density of free electrons. This has important consequences for simulations of primordial structure formation, as the ionization level determines the rate of molecular hydrogen (H_2) and hydrogen-deuterium (HD) production. These two molecules then determine the cooling time of the gas down to temperatures below 100 K. Finally, we shall also address the question of instability of radiative shocks. Chevalier & Imamura (1982) and Imamura, Wolff & Durisen (1984) found that radiative shocks with a cooling rate per unit volume $\propto\rho^2 T^\alpha$ (where ρ is the mass density, and T the temperature) are unstable against perturbations when $\alpha \leq 0.4$. This instability results in periodic oscillations of the position of the shock front and of the jump temperature at the shock front. We address the nature of these oscillations in the context of galaxy formation using a cooling

★ E-mail: rogerh@pact.cpes.susx.ac.uk

function composed of the sum of a number of terms, each with a different power law.

2 ANALYTIC PROFILES

Shocks can be generally classified into three types, depending upon the amount of cooling present. In adiabatic shocks the shocked gas does not cool significantly. Isothermal shocks have the same jump conditions at the shock front as an adiabatic shock, but the cooling is very rapid so that the downstream gas is at the same temperature as the upstream gas. Any cooling tail is thus very narrow. In between these two extremes is the case where the shocked gas has a cooling time comparable to the other time-scales of interest in a given situation.

For an adiabatic shock, the conservative form of the fluid equations in the absence of sources which change mass, momentum or energy can be written as

$$\frac{\mathrm{d}}{\mathrm{d}x}(\rho u) = 0, \tag{2}$$

$$\frac{\mathrm{d}}{\mathrm{d}x}(\rho u^2 + P) = 0, \tag{3}$$

$$\frac{\mathrm{d}}{\mathrm{d}x}\left[\rho u\left(\frac{1}{2}u^2 + \epsilon + \frac{P}{\rho}\right)\right] = 0, \tag{4}$$

where the variables u, x, ρ, ϵ and P represent velocity, position, density, specific energy and pressure respectively, all evaluated in the rest frame of the shock.

If we apply equations (2)–(4) to gas far upstream and write its properties in terms of gas far downstream, we arrive at the Rankine–Hugoniot jump conditions:

$$\rho_2 u_2^2 + P_2 = \rho_1 u_1^2 + P_1, \tag{5}$$

$$\rho_2 u_2 = \rho_1 u_1, \tag{6}$$

$$\frac{1}{2}u_2^2 + \frac{\gamma}{\gamma - 1}k_\mathrm{b}\frac{T_2}{\mu m_\mathrm{H}} = \frac{1}{2}u_1^2 + \frac{\gamma}{\gamma - 1}k_\mathrm{b}\frac{T_1}{\mu m_\mathrm{H}}, \tag{7}$$

where T is the gas temperature, k_b the Boltzmann constant μ the mean molecular weight, and m_H the mass of a hydrogen atom. The suffixes 1 and 2 refer to the upstream and downstream gas respectively, and the equation of state of the gas is given by the equations

$$\frac{P}{\rho} = \frac{k_\mathrm{b}T}{\mu m_\mathrm{H}}, \tag{8}$$

$$\epsilon = \frac{1}{\gamma - 1}\frac{k_\mathrm{b}T}{\mu m_\mathrm{H}}. \tag{9}$$

Taking $\gamma = 5/3$, we can write the pressure of the shocked gas as

$$P_2 = \frac{(4\rho_2 - \rho_1)}{(4\rho_1 - \rho_2)}P_1. \tag{10}$$

For the case of an isothermal shock where the temperature of the gas far downstream is equal to its temperature upstream, the conservation of energy equation is no longer valid and should be replaced with the condition $T_1 = T_2$. We stress, however, that the gas will still undergo an adiabatic jump at the shock front before cooling back down to its upstream temperature.

For the case of a radiative shock we wish to determine the path between the state of the gas at the shock front and its state downstream. In order to do this, we must add a cooling term to the energy flux equation:

$$\frac{\mathrm{d}}{\mathrm{d}x}\left[\rho u\left(\frac{1}{2}u^2 + \epsilon + \frac{P}{\rho}\right)\right] = -C, \tag{11}$$

where C is the emissivity. The cooling term serves to determine the path between the down-stream and adiabatic jump conditions, but does not change them in any way. Equations (2), (3) and (11) can be numerically integrated for any cooling function resulting in an analytic profile from the specified downstream conditions to the shock front. The shock front is reached when the adiabatic jump condition of equation (10) is satisfied.

3 SHOCK-TUBE

3.1 Description of the code

The shock-tube simulations were performed using a smoothed particle hydrodynamics code. The code was that described by Couchman, Thomas & Pearce (1995), but with modified geometry to make the simulation volume cuboidal with dimensions of $6 \times 6 \times 100$. The shock front was initially set to be at z coordinate 50 with gas flowing in the z direction. On what will be the upstream side of this point, particles are placed one per unit volume and given unit mass. On the downstream side, particles were placed four per unit volume. Their mass, however, is allowed to vary in order for the gas to have any density profile that is initially desired. The density profile, along with the temperature and velocity of the gas, is read in at the start of a simulation. For this geometry the simulation thus starts with 9000 particles. The particles on each side of the shock front were allowed to relax independently to a glass-like initial state.

The sides of the simulation box were periodic, with the exception of each end, where gas was fed into the box at the appropriate rate upstream and removed from the simulation a sufficient distance downstream so as not to affect any cooling tail. A padding region of two mesh cells at each end was necessary, and gas within this region had its position updated on each time-step, but did not have its energy, velocity or density updated. (The code searches for 32 neighbours, thus needing a search radius of approximately 2 units when particles are located one per cell. It is this distance that determines the size of the padding region, as any particle closer than this distance to the end of the simulation volume would experience a non-symmetric force.) All simulations were performed in the rest frame of the shock, and the units the code used were dimensionless until a cooling function was chosen.

The cooling function, and ionization/recombination rates were integrated using RK4 from Press et al. (1992), this routine being called at the end of each time-step.

4 STABLE IN-SHOCK COOLING

4.1 Theory

We write $C = n^2\Lambda$, where n is the total number density of all particle species for a fully ionized gas. (We take $n = \rho/10^{-24}\,\mathrm{g}$, corresponding to a cosmic mix of elements.) The cooling function for objects with high virial temperatures (above $10^4\,\mathrm{K}$) collapsing after the Universe has been enriched with metals can be written as the sum of three terms: a bremsstrahlung term, Λ_1, a metal line-cooling term, Λ_2, and a H-He term, Λ_3. The fit for each term is split into two temperature regimes. For $T > 10^5\,\mathrm{K}$ we have, where $\lambda = \Lambda/\mathrm{erg\,cm^3\,s^{-1}}$,

$$\lambda_1 = 5.2 \times 10^{-28}(T/\mathrm{K})^{\frac{1}{2}}, \tag{12}$$

$$\lambda_2 = 1.7 \times 10^{-18}(T/\mathrm{K})^{-0.8}Z/\mathrm{Z}_\odot, \tag{13}$$

$$\lambda_3 = 1.4 \times 10^{-18}(T/\mathrm{K})^{-1}. \tag{14}$$

For $10^5 > T > 10^4$ K we have

$$\lambda_1 = 0, \tag{15}$$

$$\lambda_2 = 1.7 \times 10^{-27} (T/\mathrm{K}) Z/Z_\odot, \tag{16}$$

$$\lambda_3 = 1.4 \times 10^{-28} (T/\mathrm{K}), \tag{17}$$

where $Z/Z_\odot$ is the metallicity in terms of solar. Here we set $Z/Z_\odot = 0.5$

The above cooling function is a good approximation to within a factor of 2 to that of Raymond & Smith (1977). The nature of this cooling function is such that the cooling rate rises abruptly as one moves from 10^4 to 10^5 K, then decreases, reaching a minimum at about 2×10^7 K. At this point, bremsstrahlung cooling starts to become effective, and the cooling rate begins slowly to rise once more as the temperature increases further. For gas being shocked from 10^4 K to a temperature of order 2×10^7 K the cooling function is of a suitable nature to produce a significant reduction in the cooling time of shocked gas, if in-shock cooling is present. The cooling rate being most rapid at lower temperatures and then decreasing as the temperature rises above 10^5 K means that a modest reduction in the maximum temperature reached could make a significant difference to the cooling time, as it is the hottest gas that takes the longest to cool. Unfortunately, a declining cooling function makes the shock unstable (see Section 6), and in this section we restrict ourselves to studying shocks which do not reach the declining part of the cooling function, and which thus settle down into a steady state.

The nature of such shocks can be specified by the ratio of the cooling time to the shock crossing time. If the cooling time is very long, and the ratio is thus large, the effect of in-shock cooling will be negligible. Conversely, if the cooling time is very rapid, in-shock cooling will tend to drive the shock towards an isothermal transition. The cooling time will be determined by the physical condition of the gas – its density and temperature. However, the shock crossing time will depend upon the mass resolution of the code, and will vary as the cube root of the particle mass.

4.2 Methodology

By specifying the downstream conditions of the shock, equations (2), (3) and (11) were numerically integrated for Λ of Section 4.1, and a profile of the cooling tail was obtained. The integration was stopped at the shock front, when equation (10) was satisfied. This profile was then read directly into the shock-tube to create the initial conditions, with the shock front being placed at the boundary between the low- and high-mass particles. Particles within the region of the cooling tail had their temperature, velocity and mass adjusted to recreate the analytic shock profile. The simulations were then allowed to run until a steady state situation was reached.

The upstream gas was started with a temperature of 5.95×10^4 K, and the analytic jump temperature was 1.84×10^5 K. The density of gas far downstream had a density 12 times that of the upstream gas. Two simulations were run with different mass resolutions: one with a ratio of the shock crossing time to the cooling time of 8, and the other with a ratio of 1.2.

4.3 Results

Figs 1 and 2 show the temperature profiles as a function of position for two shocks with ratios of 8 and 1.2 respectively. Despite the upper part of the theoretical shock being in the unstable regime, the simulations were found to settle down into a steady state. This was aided by in-shock cooling, which reduces the maximum temperature reached. The solid lines in show the analytic temperature profiles. We can see that the maximum temperature obtained is approximately 25 per cent lower than the analytic jump temperature in Fig. 1, and 50 per cent lower for the simulation in Fig. 2 which has a particle mass 512 times greater.

The effect that these reductions in jump temperature have on the cooling tails can be seen to be somewhat erratic. In both cases the cooling time of the gas decreases by a factor of approximately 2, but the spatial extent of the cooling tail depends upon the resolution. The reason for this is that spatial location is not an accurate indication of the cooling time, as the latter is dependent upon the density. We would not necessarily expect the shock-tube simulations to have the same density profile or the same density jump at the shock front as the theoretical profile. However, they do converge to the correct jump conditions far downstream.

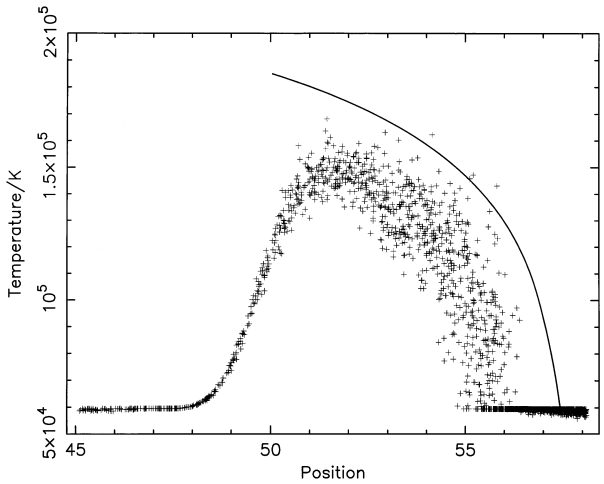

Figure 1. Steady state temperature profile demonstrating in-shock cooling. The solid line shows the analytic profile that would be expected in the absence of in-shock cooling. The ratio of the cooling-time to shock crossing time is of order 8.

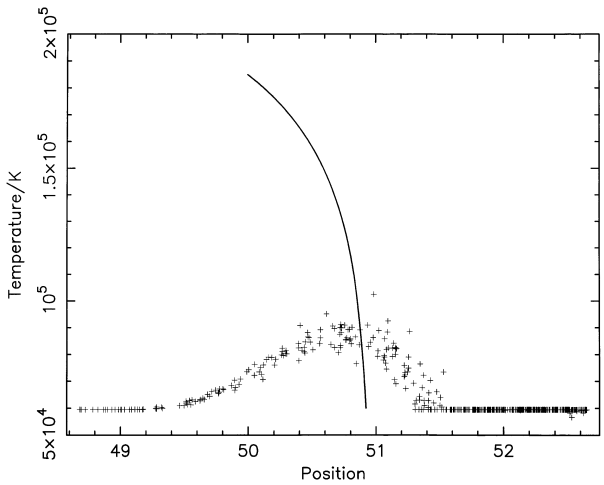

Figure 2. Steady state temperature profile demonstrating in-shock cooling. The solid line shows the analytic profile that would be expected in the absence of in-shock cooling. The ratio of the cooling-time to shock crossing time is of order 1.2.

4.4 Discussion

The effects of in-shock cooling are applicable to simulations of galaxy formation where by definition the cooling time is of order the dynamical time. A typical simulation with a dark-matter particle mass of $3 \times 10^{10}\,\mathrm{M}_{\odot}$ has a ratio of cooling time to shock crossing time of 1.2, resulting in a reduction of 50 per cent to the maximum temperature reached and a reduction in the cooling time of a factor of 2. Increasing the mass resolution by a factor of 1000 improves the situation. However, even in this case the maximum temperature reached will be 25 per cent lower than expected, and the cooling time still reduced by approximately a factor of 2.

5 SIMULATIONS WITH ELECTRON COOLING

5.1 Theory

The most important cooling mechanisms for a primordial gas with a temperature in the range 10^4–2×10^5 K are collisional excitation or ionization of neutral hydrogen by collisions with free electrons, followed by the emission of a photon. The cooling terms, taken from Haiman, Thoul & Loeb (1996), are of the form $C = n^2\Lambda$ with units of erg cm^{-3} s^{-1}:

$$C = 7.5 \times 10^{-19} \left(1 + T_5^{\frac{1}{2}}\right)^{-1} \exp\left(\frac{-1.18348}{T_5}\right) n_{\mathrm{e}} n_{\mathrm{H,}} \tag{18}$$

$$C = 4.02 \times 10^{-19} \left(\frac{T_5^{\frac{1}{2}}}{1 + T_5^{\frac{1}{2}}}\right) \exp\left(\frac{-1.57809}{T_5}\right) n_{\mathrm{e}} n_H, \tag{19}$$

where n_{e}, n_H, n_{H^+} are the number densities of free electrons, neutral hydrogen and hydrogen ions respectively in units of cm^{-3}, and T_5 is the temperature in units of 10^5 K. The rate of energy loss from the gas is proportional to the number density of free electrons. The ionization level thus needs to be known, and is generally not equal to its equilibrium value for the situations we shall consider. In order to trace the ionization level, we need to specify the ionization and recombination rates. For the purpose of this section we consider a gas composed entirely of hydrogen which is ionized through the reaction

$$\mathrm{H} + \mathrm{e}^- \mapsto \mathrm{H}^+ + 2\mathrm{e}^-, \tag{20}$$

which proceeds at a rate (Cen 1992)

$$\frac{\gamma_{\mathrm{i}}}{\mathrm{cm}^3\,\mathrm{s}^{-1}} = 1.85 \times 10^{-8} \frac{T_5^{1/2}}{1 + T_5^{1/2}} \exp\left(\frac{-1.578091}{T_5}\right). \tag{21}$$

The gas recombines via the reaction

$$\mathrm{H}^+ + \mathrm{e}^- \mapsto \mathrm{H} + h\nu, \tag{22}$$

which proceeds at a rate (Hutchins 1976)

$$\frac{\gamma_r}{\mathrm{cm}^3\,\mathrm{s}^{-1}} = 1.19 \times 10^{-13} T_5^{-0.64}. \tag{23}$$

5.2 Methodology

For the electron-cooling runs, the gas was started with jump conditions for a perfectly isothermal shock. The motivation for this approach is that the cooling time is short, meaning that the perfectly isothermal conditions are reasonably close to the stable profile and should soon evolve to that state. The mass of the downstream particles was adjusted so that the correct density jump was obtained, and the simulations were then allowed to run until the developing temperature, density and ionization profiles reach a stable state. Gas upstream had an ionization level of 4×10^{-4} and a temperature of 12 000 K, which was the minimum temperature permitted in the simulations. Gas at or below 12 000 K did not have its ionization level updated and was not allowed to cool further, as this would slow down the code too much. Instead, cooling below 12 000 K was estimated analytically.

Run 1 is a fiducial run with units designed to represent an object at a redshift of 20 containing 10^6 particles with a total baryonic mass of $4 \times 10^8\,\mathrm{M}_{\odot}$ and a virial temperature of 78 000 K. Runs 2 and 3 have the same mass resolution as the fiducial run, but represent objects with higher and lower virial temperatures respectively. Runs 4 and 6 have the same virial temperature as the fiducial run, but lower and higher mass resolution respectively. Runs 5 and 7 have a lower virial temperature than the fiducial, but different mass resolutions. The mass resolution is represented by the number of particles an object of mass $4 \times 10^8\,\mathrm{M}_{\odot}$ would contain, although the simulations which have been performed have the same number of particles in every case.

Table 1. Steady state properties of shock-tube simulations with cooling due to collisional excitation of free electrons with neutral hydrogen.

Run No.	N_{obj}	T_{a}/K	T_s/T_{a}	x_{a}	x_s/x_{a}	τ_s/τ_{a}	$\tau_{\mathrm{sf}}/\tau_{\mathrm{af}}$	$\mathrm{H}_{2,s}/\mathrm{H}_{2,a}$
1	10^6	78 000	0.27	0.14	0.11	236	2.14	0.50
2	10^6	168 000	0.15	0.58	0.08	512	2.01	0.51
3	10^6	39 000	0.45	0.029	0.24	48	1.74	0.61
4	10^3	78 000	0.22	0.14	0.09	941	2.40	0.45
5	10^3	39 000	0.44	0.029	0.16	139	2.10	0.52
6	10^9	78 000	0.39	0.14	0.24	42	1.63	0.64
7	10^9	39 000	0.81	0.029	0.41	9	1.40	0.74

5.3 Results

Table 1 lists the results of seven shock-tube simulations using the cooling functions of equations (18) and (19). From left to right, the column headings are: run number; the number of particles an object of mass $4 \times 10^8\,\mathrm{M}_{\odot}$ would contain, N_{obj}; the (analytic) virial temperature T_{a} (the temperature the shocked gas should jump to); the ratio of the maximum temperature obtained in the simulations to the virial temperature, T_s/T_{a}; the analytic ionization level for gas cooling from the virial temperature to 12 000 K, x_{a}; the ionization level of gas in the simulation that has cooled back to 12 000 K divided by the analytic level, x_s/x_{a}; the ratio of the simulated to analytic cooling times from the peak of the shock, down to 12 000 K, τ_s/τ_{a}; the ratio of the numerical to the analytic cooling times to reach 600 K, $\tau_{\mathrm{sf}}/\tau_{\mathrm{af}}$; and the ratio of the numerical to the analytic H_2 fractions at 600 K, $\mathrm{H}_{2,s}/\mathrm{H}_{2,a}$.

The analytic ionization level at 12 000 K, x_{a}, assumes an adiabatic shock followed by rapid cooling, and was calculated by integrating the shock conservation equations (2), (3) and (11) with the cooling functions of equations (18) and (19) using non-equilibrium chemistry. Cooling below 12 000 K was calculated allowing the gas to cool at a constant density to 600 K via the H_2 cooling mechanism. A detailed treatment of the gas chemistry was used incorporating formation and destruction of H_2, ionization and recombination, the cooling functions of equations (18) and (19), and the H_2 cooling function. The destruction and cooling rates of

H_2 were taken from Martin, Schwarz & Mandy (1996). The simulated cooling time from 12 000 K to 600 K, τ_{sf}, and H_2 fraction, H_{2s}, use x_s as the starting ionization level; τ_{af} and H_{2a} use x_a as the input ionization.

5.4 Discussion

5.4.1 Fiducial run

The effect of in-shock cooling is dramatic and striking in the fiducial run. The maximum temperature the shock reaches is only 0.27 of its theoretical value. This leads to an increase in the cooling time for the gas to cool back down to 12 000 K by an astonishing factor of 236. This is because the ionization levels and gas densities are both lower in the simulation than in the theoretical profile. The consequences of this are of extreme importance, as simulations of such objects will be meaningless unless in-shock cooling can be removed, since the increase in the cooling times of such objects will slow the collapse.

Also of importance is the ability of an object to cool to temperatures below 12 000 K, when molecular hydrogen becomes the dominant coolant. Molecular hydrogen is formed via the reactions

$$H + e^- \mapsto H^- + h\nu,$$

$$H^- + H \mapsto H_2 + e^-.$$

Its production is thus proportional to the ionization level, the free electrons acting as a catalyst. The effect of in-shock cooling on the fiducial run was found to halve the H_2 abundance and to increase the cooling time from 12 000 to 600 K by a factor of 2.14.

5.4.2 Effect of virial temperature

Increasing the shock jump temperature, whilst retaining the same spatial and mass resolution, results in a decrease of both the fractional temperature and the maximum ionization level reached. However, due to the complex interaction between reaction rates and cooling times, these trends do not carry over to the cooling times and H_2 abundances.

5.4.3 Effect of resolution

As one might expect, improving the mass resolution reduces the severity of any in-shock effects. As the mass resolution is improved, there is a steady convergence towards the correct values of the H_2 abundance, the cooling time to 600K, the cooling time from the virial temperature to 12 000 K, and the jump temperature. Essentially the convergence of the first three is determined by the convergence towards the correct jump temperature, as it is this temperature that determines the extent to which the gas is re-ionized, which in turn determines the rate of H_2 production and the cooling time. However, even if an object were to contain 10^9 particles, the effects of in-shock cooling would still remain significant, most noticeably for τ_s/τ_a. Such resolutions are at present not possible, and even if they were, the quantities we have considered are yet to converge. We must conclude that the resolution of typical simulations being performed is hopelessly inadequate and, if sensible results are to be obtained, a way of removing in-shock cooling must be found.

6 TEMPERATURE OSCILLATIONS OF UNSTABLE SHOCKS

6.1 Theory

For a planar radiative shock with a cooling function $\Lambda \propto T^{\alpha}$, Chevalier & Imamura (1982) showed that for $\alpha \leq 0.4$ the shock is unstable against perturbations and will undergo oscillations both spatially and in the jump temperature. The latter results from the fact that as the shock front moves, the relative velocity of the upstream gas in the frame of the shock varies. This in turn results in a different solution of the jump equations. The situation is similar for stable shocks also: if perturbed, they also undergo oscillations but with a decaying amplitude. For values of α between -1 and 2, Chevalier & Imamura found the frequency of oscillation, ω, to vary between 0.26 and 0.31 with units of $u_{in}/\bar{x}_s$, where $\bar{x}_s$ is the mean distance from the shock front to the point upstream where the gas has cooled to its upstream temperature, and u_{in} is the velocity of the upstream gas. The maximum displacement of the shock front from its mean position, x_{max}, was also calculated, and was found to be $x_{max} = \tau_{cool} v_s$, where τ_{cool} is the steady state cooling time, and v_s the speed the shock front is moving at.

6.2 Methodology

The following simulations verify the instabilities found by Chevalier & Imamura (1982) for the case of a realistic cooling function composed of a number of power-law terms (some of which are stable). An analytic profile of the cooling tail was calculated as in Section 4.2. The gas upstream had a temperature of 50 000 K, with a density jump of 100 for the downstream gas. This results in a temperature jump of a factor of 19.7 to 9.8×10^5 K. The cooling function used was that of Section 4, meaning that gas with a temperature above 10^5 K is in the unstable regime. The fact that the shock is unstable means that a steady state will never be reached, so the simulation was ran until the nature of the oscillations became apparent.

6.3 Results

The unstable nature of both the position and jump temperature of radiative shocks is well demonstrated upon consideration of Figs 3 and 4. Although the cooling function used is not strictly a power law, but rather a combination of power laws, we find that both the magnitude of the spatial oscillations, and their period, are in reasonable agreement with the work of Chevalier & Imamura as presented above. The frequency of oscillations ω was found to be $\omega = 0.31$, in agreement with the results of Imamura et al. (1984). The maximum displacement of the shock was found to be $x_{max} = 8.0$, which agrees well with the theoretical value of $x_{max} = 7.8$.

The effects of in-shock cooling on the simulations is uncertain but, given that we know it is present, it may account for the extreme oscillations down to an isothermal transition as seen in Fig. 5. We note, however, that the period and spatial magnitude of the oscillations appears to be correct even when in-shock cooling is present. In the absence of in-shock cooling, any halo with a virial temperature of more than a few times 10^5 K (i.e., galaxies) will be subject to such an instability.

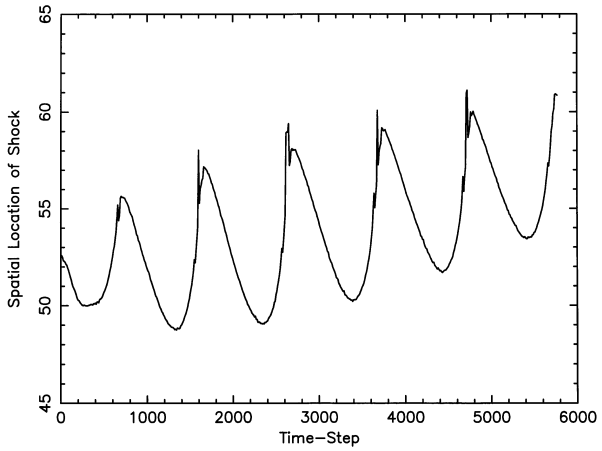

Figure 3. Position of shock front as a function of time for an unstable radiative shock.

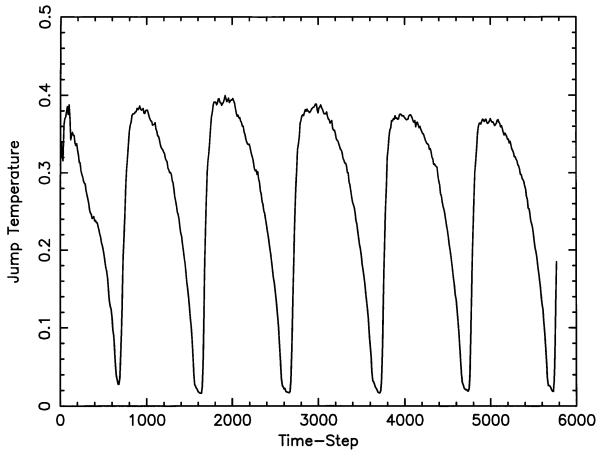

Figure 4. Oscillations of the jump temperature of an unstable shock as a function of time.

6.4 Discussion

Simulations involving unstable shocks are common. However, the fact that the shocks are indeed unstable is a little-known phenomenon. We have shown that the effect of the instability can have enormous consequences regarding interpretation of the results of such simulations. Most importantly, the temperature at the peak of the shock in two different simulations could differ by a factor of 20, and yet be completely consistent with one another.

The effect of in-shock cooling upon unstable shocks is hard to access. It is undoubtedly present, and may be responsible to some degree for the large range of jump temperatures obtained. To investigate this matter, it would be necessary to remove the effect. However, as will be discussed in the conclusions, this is no easy matter.

7 CONCLUSIONS

In this paper we have clearly demonstrated that in-shock cooling has important consequences for numerical simulations of galaxy formation, especially at high redshifts, but also for galaxies with higher virial temperatures collapsing at lower redshifts.

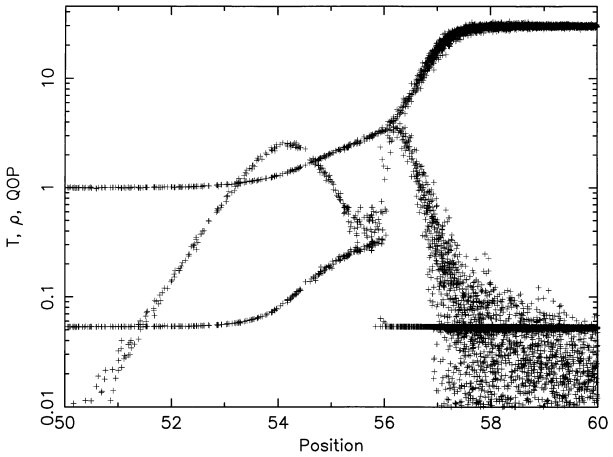

Figure 5. Graph showing the properties of temperature, density and the ratio of the artificial pressure to the pressure for a shock where in-shock cooling has been removed. The temperature starts at 0.054 and increases to 0.30 at position 56, this temperature being the correct jump temperature. The gas then cools extremely rapidly back down to its upstream value. The density starts at 1 and increases as the gas shocks and cools until it reaches its downstream value of 12. The ratio q/p has a double-peaked structure, each peak being caused by shock heating and rapid cooling respectively.

The effect of in-shock cooling on a stable radiative shock was found to decrease the maximum temperature reached by 25 per cent when the ratio of the cooling-time to shock crossing time was 8. This value increased to 50 per cent for a ratio of 1.2. The result of this was that the profiles of the cooling tails were found to have different spatial extents from the theoretical profile. From this we conclude that although the effects of in-shock cooling are quite small, the collapse rate of such objects could be altered along with the spatial extent of any cooling tail.

The effect on primordial objects of in-shock cooling was found to be extremely significant: the ionization level emerging from the shock was significantly lower by a factor of 2.4 in the best resolved case, and up to a factor of 12.1 in the worst case. The implications for the cooling time of the gas ranged from an increase of a factor of 9 up to nearly 1000, for the cooling times above 12 000 K. Below 12 000 K the result was less extreme, ranging from factors of 1.4 to 2.4. This difference is nevertheless important, and will significantly slow the collapse of any object. The resulting molecular hydrogen abundance of the gas after it was allowed to cool to 600K was found in all cases to decrease from its analytic value by a factor of around 2.

For the case of an unstable shock we find oscillations of the spatial location of the shock front and the maximum temperature reached. It is likely that the extreme oscillations of temperature observed (cooling to a virtually isothermal state) are fuelled by in-shock cooling. For the resolutions currently achievable, incorrect results will be obtained for simulations of galaxy formation.

Finally, Fig. 5 shows a successful attempt to remove in-shock cooling from the fiducial run. The method used to remove the effect was case-specific, and was achieved by allowing the gas to cool only when its temperature is in excess of the adiabatic jump temperature, or its density exceeds the adiabatic jump density. The upper curve in Fig. 5 shows the gas density, the lower curve shows the temperature, and the middle curve, with the double maximum, shows the dimensionless ratio of the artificial pressure to the pressure, q/p. The density and temperature are plotted in code units. The finite width of the shock can clearly be seen, and the

correct jump conditions and ionization level both at the peak of the shock and downstream are recovered. The correct cooling tail down to a temperature of 12 000 K is also recovered.

The importance of the ratio q/p is that it is a dimensionless indicator of when the gas is being shocked, and might therefore be used as a method of removing in-shock cooling from other simulations, by means of preventing the gas from cooling when q/p exceeds a certain threshold value (i.e., when the gas is being shocked). However, this approach is unlikely to prove successful for two reasons. First, consideration of the double-maximum structure of q/p as seen in Fig. 5 means that gas which is shocking does not necessarily have a value of q/p greater than gas which is not. Indeed, gas which is radiating rapidly (which is the case for gas whose density is increasing) has values of q/p as high as gas which is being shocked. Secondly, although q/p is dimensionless, and in theory could produce a threshold value true for all scales of simulations, we would not expect the threshold value to be the same for shocks of different strengths. These two reasons rule out the use of q/p as a possible means of eliminating in-shock cooling. This was tested in a large-scale cosmological simulation. Different objects were found to have very different values of q/p, and it was obvious that there was no single value that could be used to determine when gas was being shocked.

ACKNOWLEDGMENTS

We thank Paul Nulsen for discussion about the effects of in-shock cooling. PAT is a PPARC Lecturer Fellow.

REFERENCES

Anninos P., Zhang Y., Abel T., Norman M. L., 1997, New Astronomy, 2, 209
Cen R., 1992, ApJS, 78, 341
Chevalier R. A., Imamura J. N., 1982, ApJ, 261, 543
Couchman H., Thomas P. A., Pearce F. R., 1995, ApJ, 452, 797
Haiman Z., Thoul A. A., Loeb A., 1996, ApJ, 464, 523
Hutchins J. B., 1976, ApJ, 205, 103
Imamura J. N., Wolff M. T., Durisen R. H., 1984, ApJ, 276, 667
Martin P. G., Schwarz D. H., Mandy M. E., 1996, ApJ, 461, 265
Press W. H., Teukolsky S. A., Vetterling W. T., Flannery B. P., 1992, Numerical Recepies in Fortran, 2nd edition. Cambridge Univ. Press, Cambridge
Raymond J. C., Smith B. W., 1977, ApJS, 35, 419

This paper has been typeset from a TEX/LATEX file prepared by the author.